

## Multinucleon-transfer reactions between light-heavy ions

M. Sato, M. Sasagase, Y. Nagashima, J. Schimizu, T. Nakagawa, Y. Fukuchi, and T. Mikumo

*Institute of Physics and Tandem Accelerator Center, University of Tsukuba, Ibaraki 305, Japan*

(Received 27 May 1982)

Reactions  $^{16-18}\text{O}+^{27}\text{Al}$  and  $^{19}\text{F}+^{27}\text{Al}$  are studied at about 5 MeV/nucleon.  $^{16}\text{O}+^{27}\text{Al}$  reactions are studied also at lower energies. General features of energy spectra, the most probable  $Q$  values, which show a large energy dissipation, and, in particular, angular distributions of projectilelike products are found to be very similar to those of deep inelastic collisions of heavier systems at much higher energies. All the angular distributions in  $Q$ -value intervals of 5 MeV,  $d^2\sigma/d\Omega dQ$ , exhibit forward-peaking features and are well fitted by a form  $A \exp(-\mu\theta)/\sin\theta$ . Systematics of the variation of  $\mu$  vs  $|Q|$  and the number of transferred nucleons,  $n$ , are discussed. A picture of the rotating dinucleus model is consistent with the present observations. Cross sections of isotope production have a simple relation with  $Q_{\text{gg}}$  including a nonpairing effect of the residual targetlike nucleus.

$$\left[ \begin{array}{l} \text{NUCLEAR REACTIONS } ^{27}\text{Al}(^{16}\text{O},X), E = 88, 70, 60 \text{ MeV}, ^{27}\text{Al}(^{17}\text{O},X), \\ E = 86.4 \text{ MeV}, ^{27}\text{Al}(^{18}\text{O},X), E = 88 \text{ MeV}, ^{27}\text{Al}(^{19}\text{F},X), E = 95 \text{ MeV}, \\ Z = \text{isotopes of elements from } Z = 2 \text{ to } Z \text{ (projectile), measured energy} \\ \text{spectra, } \sigma, \sigma(\theta), \text{ and } \sigma(\theta, Q). \end{array} \right]$$

## I. INTRODUCTION

Deep inelastic collisions (DIC) in nuclear reactions were first reported to occur between heavy projectiles ( $A \geq 40$ ) and heavy targets ( $A \geq 200$ ) at high energies.<sup>1</sup> (Hereafter we refer to the reactions as being in the  $H$ - $H$  system). The DIC were also found between the projectile of a light-heavy ion ( $A < 20$ ) and a heavy target (the  $L$ - $H$  system), say,  $^{16}\text{O}+^{208}\text{Pb}$  at 140 and 310 MeV,<sup>2</sup> and between a light-heavy projectile and a light-heavy target ( $A \leq 60$ ) (the  $L$ - $L$  system), say,  $^{16}\text{O}+^{27}\text{Al}$  at 90 and 100 MeV.<sup>3,4</sup>

The common properties and often the definition of DIC among these three systems are the following: The mean c.m. kinetic energy of emitted particles,  $E_f^m$  in the reaction  $A(a,b)B$ , is much smaller than the incident c.m. energy  $E_i$ , which is much higher than the Coulomb barrier in the incident channel,  $V_c^i$ .

The inelasticity of the reaction is classified according to the modified Sommerfeld parameter,<sup>5</sup>

$$\eta' = Z_a Z_A e^2 / \hbar v',$$

with

$$v' = [2(E_i - V_c^i) / \mu_i]^{1/2},$$

where  $Z_a$  and  $Z_A$  are the atomic numbers of projectile and target, and  $\mu_i$  is the reduced mass in the incident channel. In the  $L$ - $L$  system, say, for the

$^{16}\text{O}+^{27}\text{Al}$  reaction, at incident laboratory energy of 90–100 MeV,<sup>3,4</sup>  $\eta' \leq 10$ , which is much lower than in the  $H$ - $H$  and  $L$ - $H$  systems at much higher energies, e.g.,  $\eta' = 179$  for  $^{40}\text{Ar}+^{232}\text{Th}$  at 388 MeV,<sup>1</sup> and  $\eta' = 27$  for  $^{16}\text{O}+^{208}\text{Pb}$  at 305 MeV.<sup>2</sup> According to this classification based on the values of  $\eta'$ , small  $\eta'$  suggests a large degree of inelasticity, and hence the occurrence of DIC in the  $L$ - $L$  system even at relatively low incident energies.

In the reactions  $^{16}\text{O}+^{27}\text{Al}$  at 88 MeV, Mikumo *et al.* showed<sup>4</sup> that the reaction mechanism evolves from a quasielastic collision (QEC), if any, via DIC to a complete fusion (CF) with an increase in the number of transferred nucleons,  $n$ , and in the absolute value of reaction  $Q$  values  $|Q|$  ( $Q < 0$  in general). The angular distributions of reaction products as a function of  $Q$  value are expressed in the form

$$d^2\sigma/d\Omega dQ = A \exp(-\mu\theta)/\sin\theta$$

throughout a wide angular range, where  $\mu$  again reflects the degree of inelasticity for all reactions.

On the other hand, in  $^{16}\text{O}+^{27}\text{Al}$  reactions, energy spectra of all emitted particles, except for  $n = 0$  and 1, are of the form of a single bump instead of the double bumps observed in the  $H$ - $H$  and  $L$ - $H$  systems.

In order to elucidate the characteristic features of DIC in the  $L$ - $L$  system and to compare with those in the  $H$ - $H$  and  $L$ - $H$  systems, we extended the study to the reactions  $^{16-18}\text{O}+^{27}\text{Al}$  and  $^{19}\text{F}+^{27}\text{Al}$  at

around 90–100 MeV. Supplementary measurements were also made for  $^{16}\text{O}+^{27}\text{Al}$  at 70 and 60 MeV and for  $^{16}\text{O}+^{50}\text{Ti}$  at 80 MeV. The study of angular correlation between a heavy ejectile  $b$  and alpha particles of the three-body reactions

$$a + A \rightarrow b + \alpha + B$$

is reported in the following paper by Sasagase *et al.*<sup>6</sup>

## II. EXPERIMENTAL ARRANGEMENT

The experiments were performed at the Tandem Accelerator Center, the University of Tsukuba. Beams of  $^{16}\text{O}$ ,  $^{17}\text{O}$ ,  $^{18}\text{O}$ , and  $^{19}\text{F}$  from a 12 UD Pelletron Tandem Accelerator bombarded  $^{27}\text{Al}$  targets. The beams used in this experiment were the following: 88, 70, and 60 MeV for  $^{16}\text{O}$ , 60–200 nA on target produced from a sputter ion source; 86.4 MeV for  $^{17}\text{O}$ , 40 nA; 88 MeV for  $^{18}\text{O}$ , 70 nA, both obtained from an ordinary duo plasmatron using  $\text{O}_2$  gas enriched to 30% with  $^{17}\text{O}_2$  or 60% with  $^{18}\text{O}_2$  and 95 MeV for  $^{19}\text{F}$ , 50 nA from the sputter ion source using a conical target of  $\text{CaF}_2$ . The targets were self-supporting  $^{27}\text{Al}$  foils of 120–280  $\mu\text{g}/\text{cm}^2$  thicknesses, which were determined by measuring energy losses of  $^4\text{He}$  from a  $^{241}\text{Am}$  source. The uncertainty of the measurements of target thicknesses were within 6%.

Reaction products were detected by two sets of a conventional  $\Delta E$ - $E$  type of counter telescope. One consisted of 6.7  $\mu\text{m}$  thick  $\Delta E$  and 1000  $\mu\text{m}$  thick  $E$  silicon detectors, suitable for the detection of low energy (down to several MeV) products. The other consisted of 30  $\mu\text{m}$  thick  $\Delta E$  and 1000  $\mu\text{m}$  thick  $D$  detectors capable of identifying the products not only in  $Z$  [ $Z \leq Z$  (projectile)] but also in  $A$ .

The signal pairs of  $\Delta E$  and  $E$  from the detectors were accumulated in computer systems PDP 11/40 for preaccumulating, and PDP 11/50 for recording and analyzing. Particle identification was performed by the operation of selecting bands, which is a direct access to the contour map of  $\Delta E$  and  $E + \Delta E$  by use of cursor function on a keyboard. The energy of the products were calibrated by the elastic scattering measurements. Comparing with the estimation based on the available values of energy loss by Northcliffe and Schilling,<sup>7</sup> this calibration held within  $\pm 1$  MeV over the entire energy region of interest.

## III. RESULTS AND DISCUSSIONS

### A. Energy spectra of ejectiles

The energy spectra of the ejectiles of isotopes from He to O emitted at  $\theta_{\text{lab}}=22^\circ$  in the reactions  $^{18}\text{O}+^{27}\text{Al}$  at 88 MeV are shown in Fig. 1. The

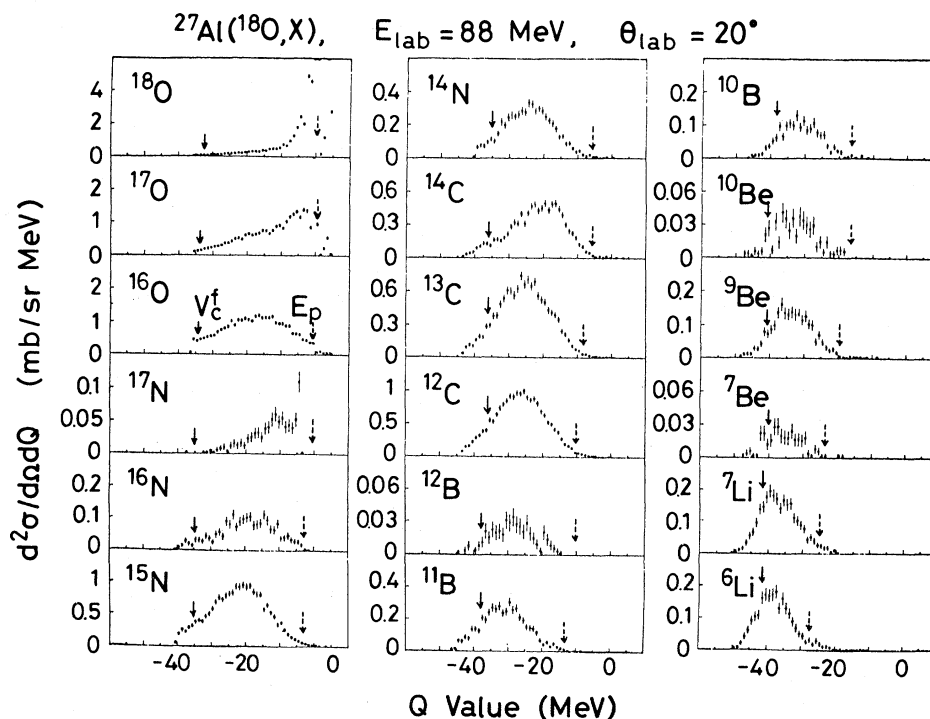


FIG. 1. Energy spectra of particles emitted from the reactions  $^{18}\text{O}+^{27}\text{Al}$  at 88 MeV,  $\theta_{\text{lab}}=20^\circ$ . The abscissa is expressed in  $Q$  values. The arrows denoted  $E_p$  and  $V_c^f$ , respectively, correspond to the velocity of the projectile and to the Coulomb barrier in the two-body exit channel, with the radius parameter,  $r_0=1.4$  fm.

abscissa is expressed in  $Q$  values assuming two-body reactions. In the spectra for  $n=0$  ( $^{18}\text{O}$ ) and  $n=1$  ( $^{17}\text{O}$  and  $^{17}\text{N}$ ), some discrete structures corresponding to ground and low-excited states of residual nuclei are observed. For  $n \geq 2$  all the spectra are of continuous structure with only one bump. In none of the cases are two bumps observed, which is in contrast with the cases of the  $H-H$  and  $L-H$  systems. The situation described above is essentially the same with other  $L-L$  systems in the present study.

For most cases, the most probably kinetic energies  $E_f^m$  of the ejectiles are much less than the incident c.m. energy  $E_i$ , i.e.,  $E_f^m \ll E_i$ , especially for large  $n$ ; hence, DIC is important according to its conventional definition of DIC. The most probable effective  $Q$  values,

$$Q_{\text{eff}}^m = E_f^m - E_i - (V_c^f - V_c^i),$$

are compared with empirical formulas given by Mikumo *et al.*<sup>4,8</sup> and the results are consistent with the formula for DIC for  $n \lesssim 8$ , i.e.,  $Q_{\text{eff}}^m = \alpha'n + \beta'$  with

$$\alpha' \simeq -0.061(E_i - V_c^i) + 0.11 \text{ (MeV)}$$

and

$$\beta' \simeq -0.37(E_i - V_c^i) - 0.51 \text{ (MeV)}$$

and not with the formula for QEC, i.e.,  $Q_{\text{eff}}^m = \alpha n + \beta$ , with

$$\alpha \simeq -0.1(E_i - V_c^i) - 0.9 \text{ (MeV)}$$

and  $\beta \simeq -3 \text{ MeV}$ .

However,  $E_f^m$  is much larger than  $V_c^f$ , which is in strong contrast with the  $H-H$  case, i.e.,  $E_f^m \simeq V_c^f$ . This feature reflects the fact that in the  $L-L$  system, the thermal equilibration in the DIC is less complete than in DIC in the  $H-H$  system, as will be discussed later in more detail.

### B. Angular distributions of ejectiles

The energy spectra of ejectiles are divided into 5 MeV bins in  $Q$  values, and the angular distributions  $d^2\sigma/d\Omega dQ$  of all  $Q$ -value bins of ejectiles in the reactions  $^{18}\text{O} + ^{27}\text{Al}$  at 88 MeV are given in Fig. 2.

All the angular distributions are well reproduced by a formula

$$d^2\sigma/d\Omega dQ = A \exp(-\mu\theta)/\sin\theta \quad (1)$$

as was reported in a previous paper for  $^{16}\text{O} + ^{27}\text{Al}$  at 88 MeV.<sup>4</sup> The dashed lines in Fig. 2 are the calculated lines obtained using Eq. (1). The uncertainty of the determination of  $\mu$  is shown for the case of  $^{15}\text{N}$  ejectiles, as is seen from lines denoted  $\mu$  and  $\mu \pm 0.3 \text{ (rad}^{-1}\text{)}$ . The same situation holds for all the incident variables in this study, i.e.,  $^{17}\text{O} + ^{27}\text{Al}$  at

86.4 MeV,  $^{19}\text{F} + ^{27}\text{Al}$  at 96 MeV, and even for  $^{16}\text{O} + ^{27}\text{Al}$  at 70 and 60 MeV, in a wide angular region. For  $^{16}\text{O} + ^{27}\text{Al}$ , the measurement was made at small angles  $\theta_{\text{lab}}$  down to  $3^\circ$  and large angles up to  $90^\circ$ . We were able to fit all the data with formula (1) in all the angular region. There is no indication of the bell-shaped angular distribution, characteristic of QEC, even at the angle much smaller than the grazing angle ( $\simeq 17^\circ$  for 88 MeV  $^{16}\text{O} + ^{27}\text{Al}$ ). Even at lower bombarding energies of 70 and 60 MeV, for  $^{16}\text{O} + ^{27}\text{Al}$  and  $^{16}\text{O} + ^{50}\text{Ti}$  at 80 MeV, no bell-shaped angular distributions were observed.

This circumstance is in strong contrast to the cases of the  $H-H$  and  $L-H$  systems. In  $^{40}\text{Ar} + ^{23}\text{Th}$  at 388 MeV,<sup>1</sup> the angular distributions of the products change from a bell-shaped form with the peak at  $\theta \simeq \theta_{\text{gr}}$  for QEC to an exponential form with the increase of the inelasticity, i.e., the increase of  $n$  and  $|Q|$ . In the case of  $^{16}\text{O} + ^{208}\text{Pb}$ ,<sup>2</sup> the angular distributions of the energy-integrated products on  $N$ ,  $C$ , and  $B$  are bell shaped at 140 MeV, whereas they are of an exponential form as given by (1) at 310 MeV.

The angular distribution of form (1) is, as discussed in a previous paper,<sup>4</sup> well explained by a rotating dinucleus system (DNS).<sup>1,9,10</sup> The projectile and the target are thought to stick to each other and form a DNS of dumbbell shape, rotating with the angular velocity  $\omega$ , and the exchange of nucleons and energies is thought to take place at the contact region of the dumbbell. After the lifetime  $\tau$  of the system, the scission of DNS occurs, producing the ejectile and the residual nucleus.

The term  $\mu$  in (1) can be understood as

$$1/\mu = \theta_d = \omega\tau, \quad (2)$$

with  $\theta_d$  the mean angle of rotation of DNS before it decays.  $\mu$  is another measure of inelasticity<sup>9,2</sup>: The smaller the value of  $\mu$ , the longer the lifetime  $\tau$ . Indeed when  $\mu$  becomes small, say, less than 0.5, the angular distribution approaches the form  $\sim 1/\sin\theta$ , a form characteristic of the complete fusion (CF). As was pointed out in a previous paper,<sup>4</sup> the reaction mechanism evolves gradually from DIC towards CF with the increase of  $n$  and  $|Q|$ , revealing little contribution of QEC in the present cases.

The reason why, in the reactions of the  $L-L$  system studied here, DIC dominates over QEC even at low bombarding energies, as can be seen in the fact that  $E_f^m \ll E_i$  and in the absence of bell-shaped angular distributions, is consistent with the classification of reaction mechanisms according to the modified Sommerfeld parameter  $\eta'$ .<sup>5</sup> In the present study  $\eta' \leq 10$ , which is much smaller than for the reactions of the  $H-H$  and  $L-H$  systems quoted above (several tens to 100).

The values of  $\mu$  for the reactions  $^{16-18}\text{O} + ^{27}\text{Al}$

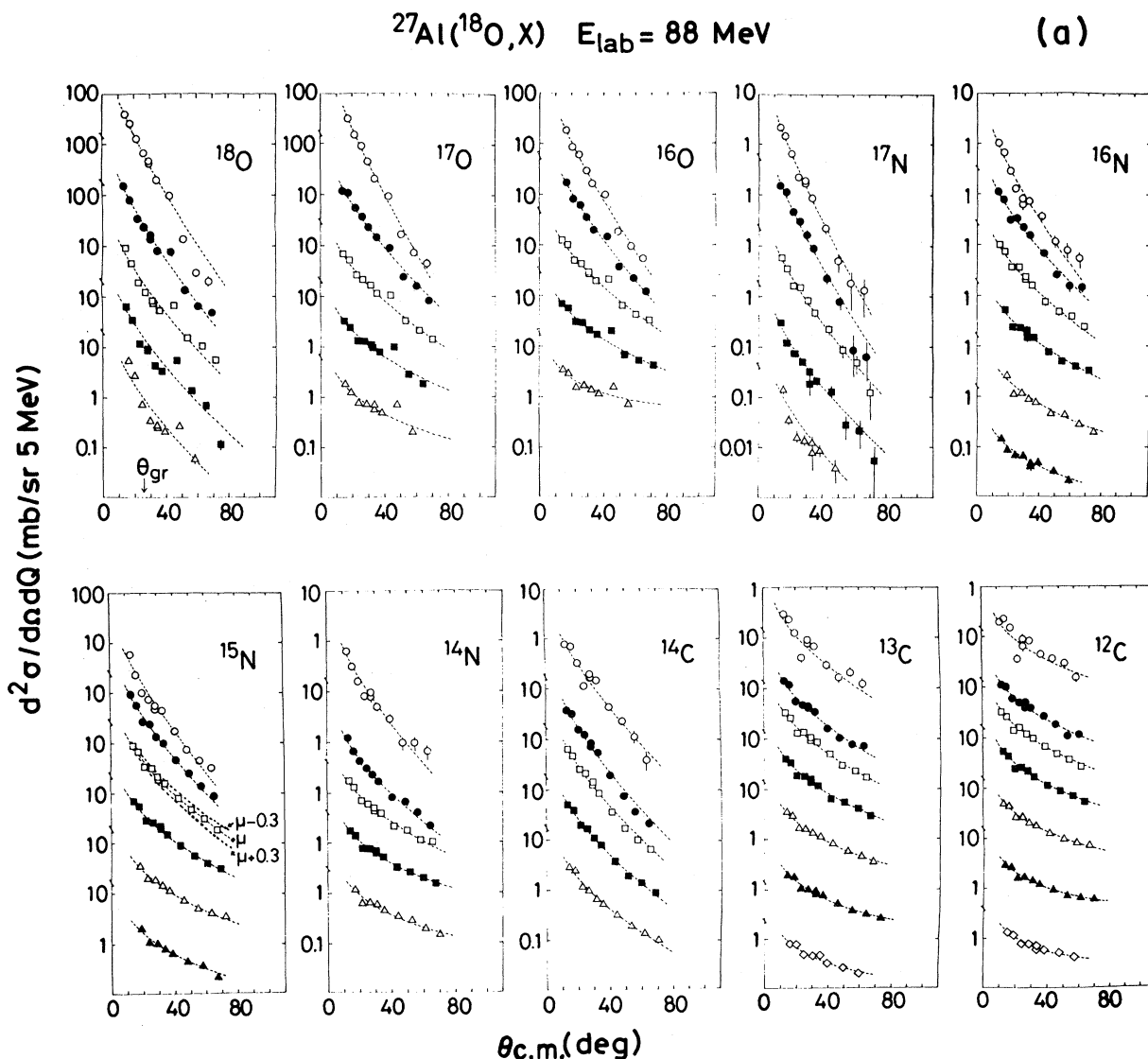


FIG. 2. Angular distributions of differential cross sections,  $d^2\sigma/d\Omega dQ$  [mb/sr  $\times$  (5 MeV)], of the reaction products in the reactions  $^{18}\text{O} + ^{27}\text{Al}$ , at 88 MeV. The  $Q$  values are divided into 5 MeV bins. The dashed lines are obtained using Eq. (1). The error in the determination of  $\mu$  ( $\text{rad}^{-1}$ ) in Eq. (1) is indicated for the case of the  $^{15}\text{N}$  ejectile:  $\circ$ :  $-10 < Q < -5$ ;  $\bullet$ :  $-15 < Q < -10$ ;  $\square$ :  $-20 < Q < -15$ ;  $\blacksquare$ :  $-25 < Q < -20$ ;  $\triangle$ :  $-30 < Q < -25$ ;  $\blacktriangle$ :  $-35 < Q < -30$ ;  $\diamond$ :  $-40 < Q < -35$ ;  $\blacklozenge$ :  $-45 < Q < -40$ ;  $\odot$ :  $-50 < Q < -45$ .

and  $^{19}\text{F} + ^{27}\text{Al}$  at  $\sim 90$  MeV are shown for typical ejectiles as a function of  $Q$  value in Fig. 3(a), and for individual cases of nucleon transfer and for  $Q$  value bins in Fig. 3(b). An example of the uncertainty for the determination of the value of  $\mu$  is shown for the reaction  $^{18}\text{O} + ^{27}\text{Al} \rightarrow ^{15}\text{N}$  in Fig. 2, as mentioned above.

Figures 3(a) and (b) show clearly that  $\mu$  decreases, in general, with the increase of  $n$  and  $|Q|$ , i.e., with

the increase of inelasticity, which is consistent with the picture of the DNS model. Certain reactions, however, have larger values of  $\mu$  even for large  $|Q|$  as compared with those producing adjacent reaction products. The contrast is the strongest for the reactions  $(^{18}\text{O}, ^{18}\text{O}')(^{17}\text{O}, ^{16}\text{N})$  and  $(^{18}\text{O}, ^{17}\text{N})$  ( $p$  transfer);  $(^{18}\text{O}, ^{14}\text{C})$  and  $(^{19}\text{F}, ^{15}\text{N})$  ( $2p2n$  transfer). These reactions are considered to hold more direct type of features even for large  $|Q|$  than the reactions pro-

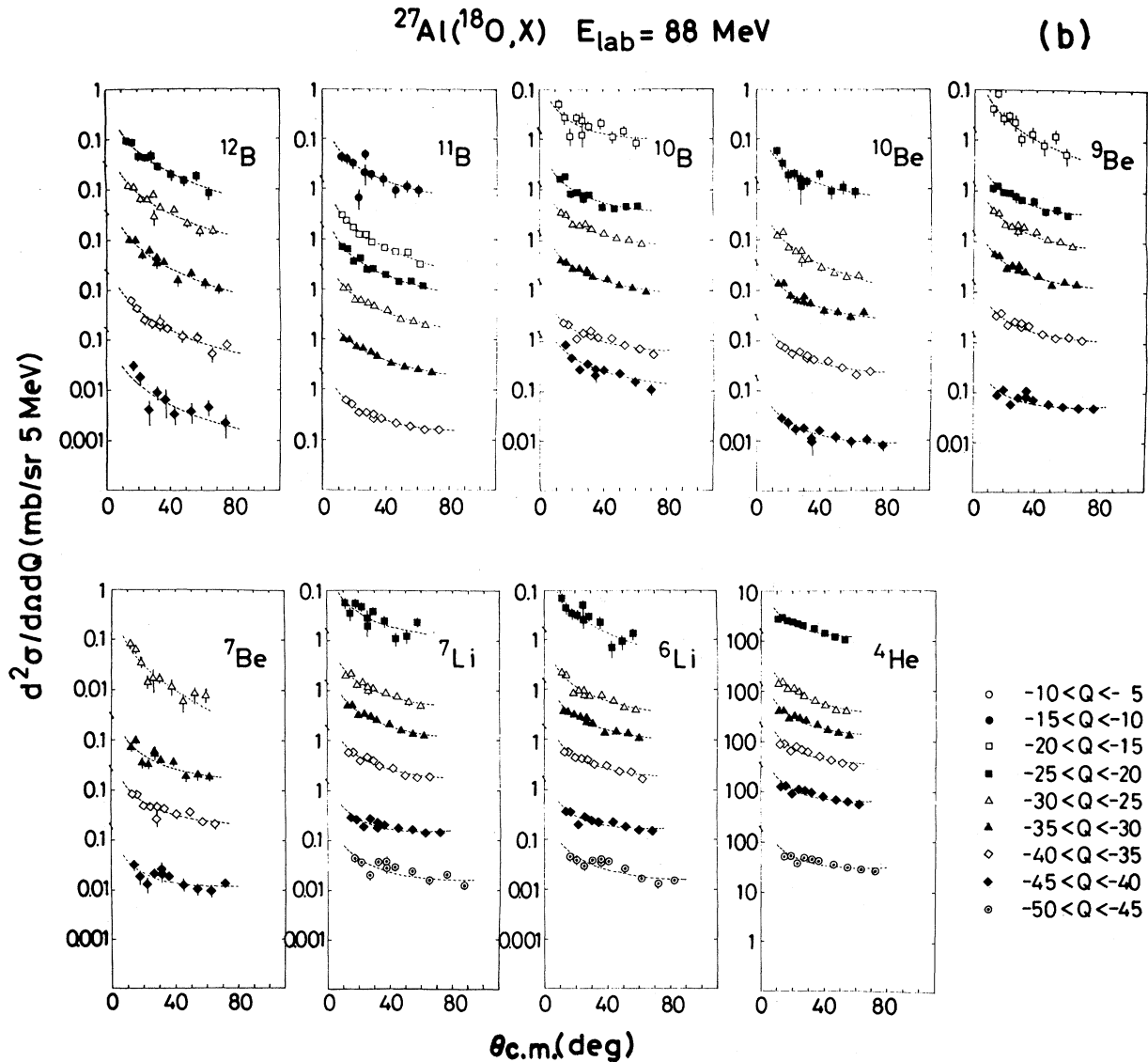


FIG. 2. (Continued.)

ducing neighboring products.

Here we mention a contour map of yields of ejectiles in the  $\theta$ - $Q$  plane like that given by Wilczyński.<sup>11</sup> An example for the case of  $^{27}\text{Al}(^{16}\text{O}, ^{12}\text{C})$  at 88 MeV is shown in Fig. 4. As is clear from the features already described, no "island" appears corresponding to QEC around  $\theta_{\text{gr}} \approx 17^\circ$  in the contour map. Instead, the maximum yields are concentrated towards  $0^\circ$  with the energy  $E_f^m$  much below  $E_i$  (the dominance of DIC), but still larger than  $V_c^f$ . (See also Fig. 1) According to Wilczyński's picture, we should conclude that the emitted particles are deflected mainly towards nega-

tive angles. This is due to the weak Coulomb repulsion in the  $L$ - $L$  system compared with the attractive nuclear force.

### C. Cross sections of isotope production

The energy-integrated cross sections  $d\sigma/d\Omega$  of the production of isotopes, measured at a specific angle, are reported to be proportional to  $\exp(Q_{gg})$  among the isotopes,<sup>1,9</sup> where  $Q_{gg}$  are the  $Q$  values of specific two-body reactions leaving both products in their ground states. This nature is well explained by

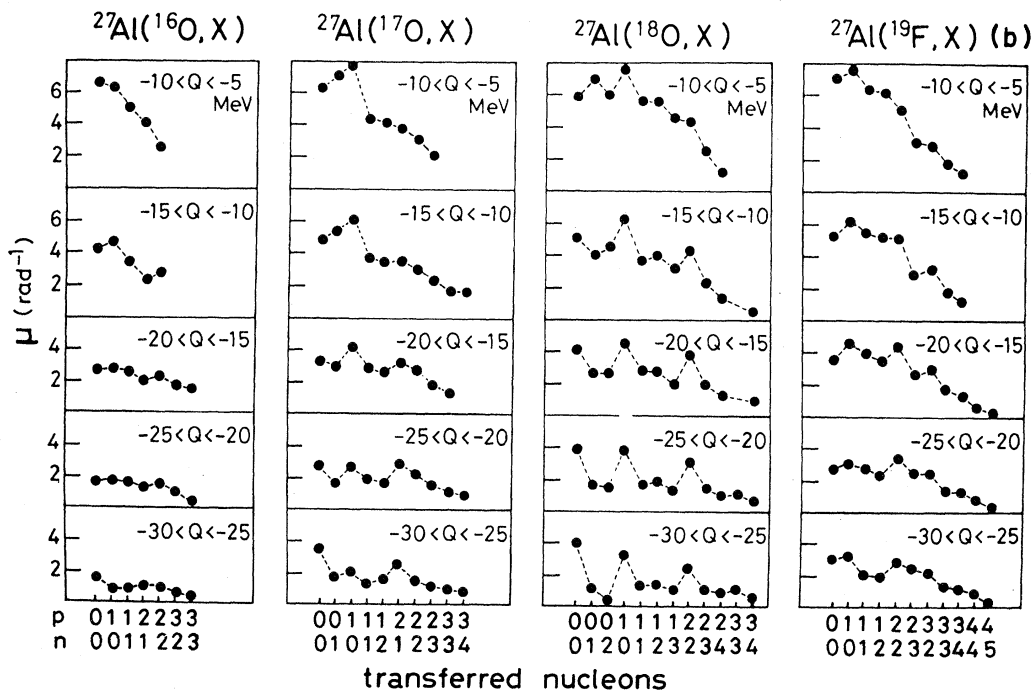
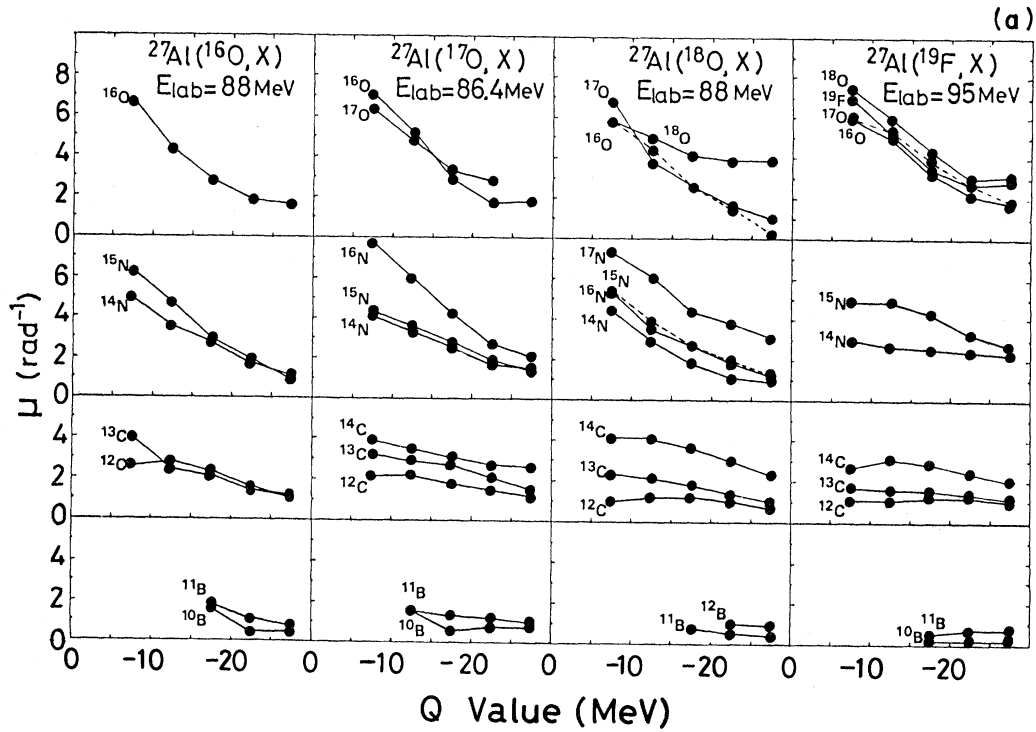


FIG. 3. The coefficient  $\mu$  ( $\text{rad}^{-1}$ ) in Eq. (1) for the reaction  $^{16-18}\text{O} + ^{27}\text{Al}$ ,  $^{19}\text{F} + ^{27}\text{Al}$  at  $\approx 5$  MeV/nucleon plotted as functions of (a)  $Q$  values for specific ejectiles, and (b) numbers of transferred protons ( $p$ ) and neutrons ( $n$ ) for specific  $Q$ -value bins.

the picture of DNS, assuming that DNS be in a thermal equilibrium with a constant temperature  $T$ , and with and without the correction due to the non-pairing effect of nucleons in the residual nucleus.

As an example of our  $L$ - $L$  system, the  $\log(d\sigma/d\Omega)$  of products of reactions  $^{18}\text{O}+^{27}\text{Al}$  measured at several angles are plotted vs  $Q_{gg}$  in Fig. 5(a) grouped together for each element. The situation appears to be very complex, changing drastically with the angles of emission, and no obvious linearity holds between  $\log(d\sigma/d\Omega)$  and  $Q_{gg}$ . The most

marked irregularity is seen for  $^{18}\text{O}$ ,  $^{17}\text{N}$ , and  $^{14}\text{C}$ . For these reaction products, the irregularity was observed with the values of  $\mu$  [Figs. 3(a) and (b)], and the reaction processes producing these products are considered to be faster than those producing adjacent isotopes.

Next, consider the correction  $\Delta(A,Z)=\delta(p)+\delta(n)$  to  $Q_{gg}$  owing to the nonpairing effect of protons and neutrons in the heavier two-body reaction residues. In Fig. 5(b)  $\log(d\sigma/d\Omega)$ 's are plotted against  $Q_{gg}+\Delta(A,Z)$ ,

$$\text{with } \Delta(A,Z) \text{ (MeV)} = \begin{cases} -33.5A^{-3/4} & \text{for } A \text{ even, } Z \text{ even,} \\ 0 & \text{for } A \text{ odd,} \\ +33.5A^{-3/4} & \text{for } A \text{ even, } Z \text{ odd.} \end{cases} \quad (3)$$

At a very forward angle, say  $\theta_{\text{lab}}=8^\circ$  or  $10^\circ$ , no exponential relation between  $d\sigma/d\Omega$  and  $Q_{gg}+\Delta(A,Z)$  is seen for O, N, and C isotopes. On the contrary, at larger angles, say  $\theta_{\text{lab}}=35^\circ$ ,  $\log(d\sigma/d\Omega)$  is almost linear to  $Q_{gg}+\Delta(A,Z)$  among the isotopes, and also the gradients are almost the same among all elements. The situation is similar for the reactions of different incident channels such as  $^{17}\text{O}+^{27}\text{Al}$  and  $^{19}\text{F}+^{27}\text{Al}$ , although the number of identified isotopes is much lower.

From these features, we conclude that except at extremely forward angles, the transfer reactions in the  $L$ - $L$  system proceed mainly via DIC, and is consistent with the formation of DNS in an intermediate stage. However, as can be seen from the fact that  $E_f > V_c^f$  as mentioned above, the thermal equi-

libration is incomplete, at least for reactions producing the ejectiles with  $Z \geq 4$ . At extremely forward angles the irregularity in Fig. 5(b) shows that some different reaction mechanism, e.g., projectile breakup, may play an important role, especially for reactions such as inelastic scattering and  $p$  and  $2p2n$  transfer. We report, in the following paper, the observation of the projectile breakup for the case of  $^{16}\text{O}+^{27}\text{Al} \rightarrow \alpha$  at 87.4 MeV.<sup>6</sup> It is also to be noted that for the reaction  $^{16}\text{O}+^{27}\text{Al}$  at 88 MeV,<sup>4</sup>  $|Q_{\text{eff}}^m|$  increases strongly with the increase of  $\theta$ , for  $\theta_{\text{lab}} \leq 30^\circ$  and for O, N, and C, but is less angle-dependent for lighter ejectiles, and changes little with  $\theta$  for  $\theta_{\text{lab}} \leq 30^\circ$  and for the lightest ejectiles.

Figure 6 shows the energy-integrated cross sections  $d\sigma/d\theta$  of isotopes emitted from the reactions  $^{18}\text{O}+^{27}\text{Al}$  at 88 MeV. Even for the energy-integrated cross sections,  $d\sigma/d\theta$  is still an exponential function of  $\theta_{\text{lab}}$  for isotopes of, say,  $Z \geq 5$  and almost isotropic for, say,  $Z \leq 4$ . Figure 7 shows  $d\sigma/d\theta$  for elemental production for the reactions  $^{16}\text{O}+^{27}\text{Al}$  at 88, 70, and 60 MeV [Fig. 7(a)] and  $^{16}\text{O}$ ,  $^{17}\text{O}$ ,  $^{18}\text{O}$ ,  $^{19}\text{F}+^{27}\text{Al}$  [Fig. 7(b)]. Vertical arrows on the abscissa in Fig. 7(a) show classical grazing angles assuming a Coulomb trajectory with a radius parameter  $r_0=1.4$  fm. The gross features of angular distributions of cross sections of elemental production are more similar to those of the  $L$ - $H$  system at high energy (310 MeV  $^{16}\text{O}+^{208}\text{Pb}$ ) than at low energy (140 MeV  $^{16}\text{O}+^{208}\text{Pb}$ ).<sup>4</sup> These figures together with Figs. 2 and 6 indicate clearly that in order to understand the details of reaction mechanisms and their evolution as functions of outgoing energies, it was crucial to identify not only  $Z$  but also  $A$  of emitted particles and to look at  $Q$ -value dependent angular distributions.

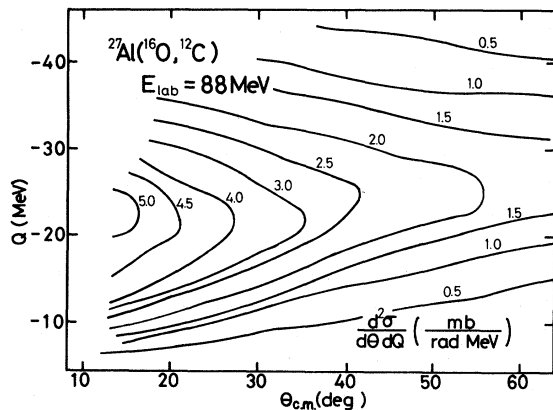


FIG. 4. Contour map of the yield  $d^2\sigma/d\theta dQ$  (mb/rad $\times$ MeV) of the reaction  $^{27}\text{Al}(^{16}\text{O},^{12}\text{C})$  at 88 MeV in the  $\theta$ - $Q$  plane.

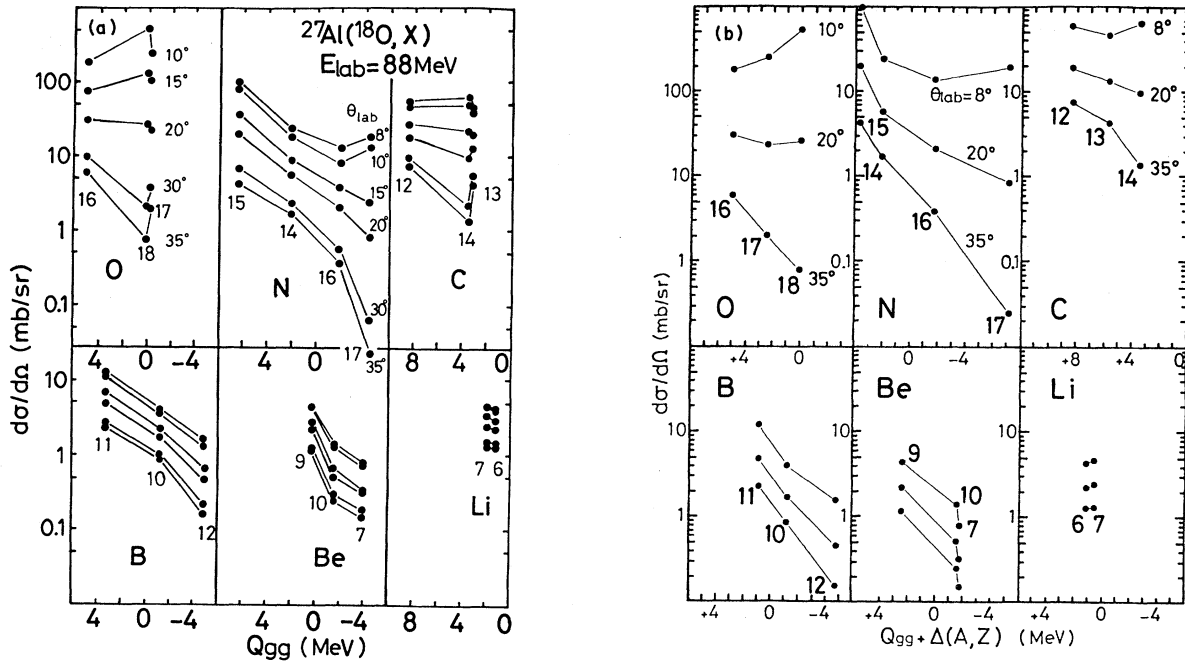


FIG. 5. Energy-integrated cross sections  $d\sigma/d\Omega$  (mb/sr) of the ejectiles of isotopes of O, N, C, B, Be, and Li in the reactions  $^{18}\text{O} + ^{27}\text{Al}$  at 88 MeV, at several angles, expressed as a function of (a) ground-state  $Q$  values,  $Q_{gg}$ , and (b)  $Q_{gg} + \Delta(A, Z)$ , where  $\Delta(A, Z)$ , defined in Eq. (3), denotes the nonpairing effect of nucleons in the heavier excited residual nuclei.

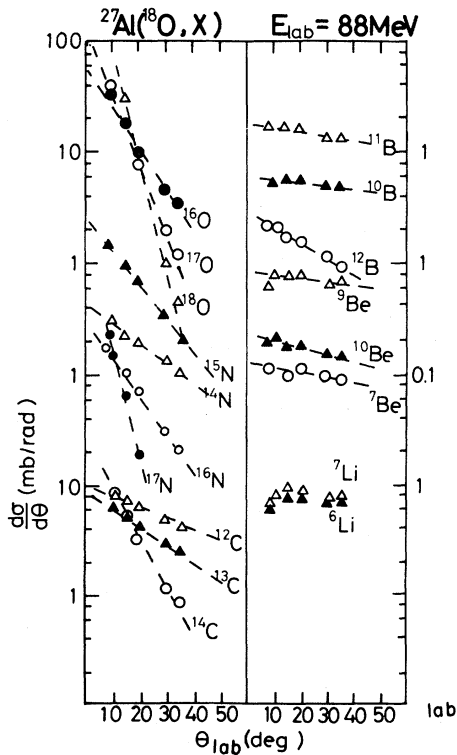


FIG. 6. Angular distribution  $d\sigma/d\theta$  (mb/rad) of energy-integrated ejectiles of isotopes from the reactions  $^{18}\text{O} + ^{27}\text{Al}$  at 88 MeV.

#### IV. CONCLUSION

Through the study of energy spectra, most probable  $Q$  values, angular distributions, and production cross sections of isotopes emitted in the  $L$ - $L$  system, we have obtained information about the reaction mechanisms of transfer reactions.

In the  $L$ - $L$  system even at relatively low energies, say, less than 100 MeV, we observed many features similar to those of DIC found in high-energy  $H$ - $H$  and  $L$ - $H$  systems. The contribution of DIC is very important compared with QEC, and the reaction mechanism evolves towards CF with the increase of  $n$  and  $|Q|$ . The yields of emitted particles are concentrated towards  $0^\circ$  with  $E_f^m \ll E_i$ , for  $Z$  (ejectile)  $\geq 4$ . This is explained by a negative angle deflection according to a Wilczyński's picture. The picture of DNS, developed to explain the DIC of the  $H$ - $H$  system at much higher energies assuming two-body reactions, is found to be consistent with the present data of the  $L$ - $L$  system. However, the thermal equilibration of DNS is less complete at least for  $Z$  (ejectile)  $\geq 4$ , as is seen from the fact that  $E_f^m > V_c^f$ . At extremely forward angles, different mechanisms without passing through the formation of DNS, such as the projectile breakup, may play an important role.

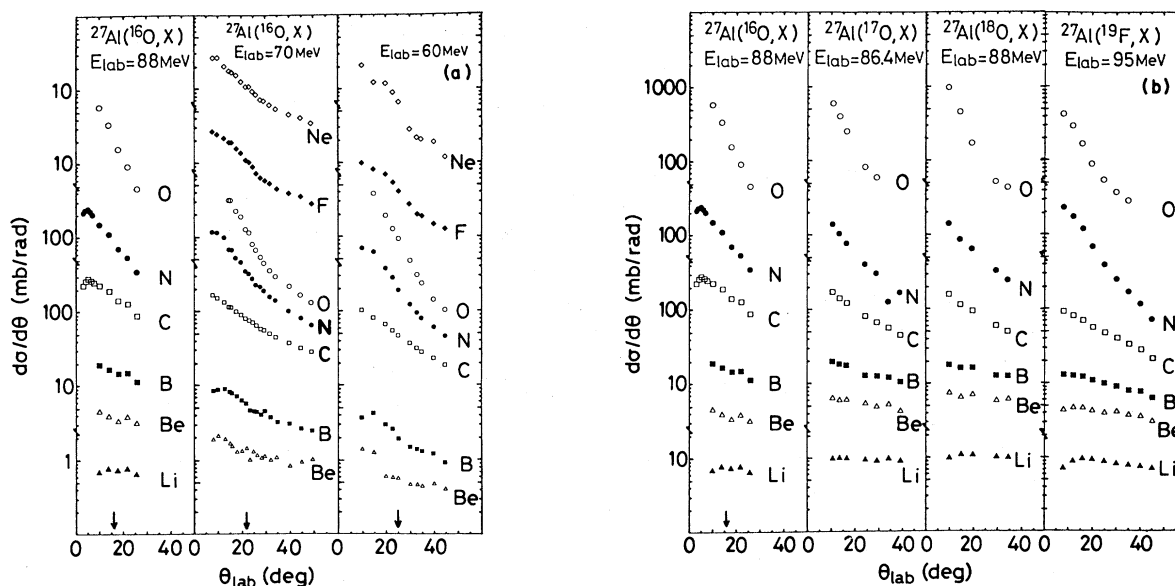


FIG. 7. Angular distributions  $d\sigma/d\theta$  (mb/rad) of elemental production in the reactions (a)  $^{16}\text{O}+^{27}\text{Al}$  at 88, 70, and 60 MeV, and (b)  $^{16-18}\text{O}+^{27}\text{Al}$ ,  $^{19}\text{F}+^{27}\text{Al}$  at  $\approx 5$  MeV/nucleon. The arrows in the figures for  $^{16}\text{O}+^{27}\text{Al}$  indicate the positions of classical grazing angles.

#### ACKNOWLEDGMENTS

The authors are grateful to Dr. K. Katori, Dr. K. Furuno, Dr. T. Nomura, Dr. S. M. Lee, and Dr. T.

Kishimoto for stimulating discussions and also to the technical staff at the Tandem Accelerator Center, the University of Tsukuba. This work was supported in part by the Nuclear and Solid State Research Project, University of Tsukuba.

- <sup>1</sup>A. G. Artukh, G. F. Gridnev, V. L. Mikkeev, V. V. Volkov, and J. Wilczyński, Nucl. Phys. **A215**, 91 (1973).
- <sup>2</sup>C. K. Gelbke, C. Olmer, M. Buenerd, D. L. Hendrie, S. Mahoney, M. C. Mermaz, and D. K. Scott, Phys. Rep. **42**, 311 (1978).
- <sup>3</sup>T. M. Cormier, A. J. Lazzarini, M. A. Neuhausen, A. Sperduto, K. Van Bibber, F. Vidabaek, G. Young, E. B. Blum, L. Herreid, and W. Thomas, Phys. Rev. C **13**, 682 (1976).
- <sup>4</sup>T. Mikumo, M. Sasagase, M. Sato, T. Ooi, Y. Higashi, Y. Nagashima, and M. Yamanouchi, Phys. Rev. C **21**, 620 (1980).
- <sup>5</sup>J. Galin, J. Phys. (Paris) C **5**, **37**, 83 (1976).

- <sup>6</sup>M. Sasagase, M. Sato, S. Hanashima, K. Furuno, Y. Nagashima, Y. Tagishi, S. M. Lee, and T. Mikumo, Phys. Rev. C **27**, 2630 (1983).
- <sup>7</sup>L. C. Northcliffe and R. F. Schilling, Nucl. Data Tables **A7**, 233 (1970).
- <sup>8</sup>T. Mikumo, T. Kohno, K. Katori, T. Motobayashi, S. Nakajima, M. Yoshie, and H. Kamitsubo, Phys. Rev. C **14**, 1458 (1976).
- <sup>9</sup>V. V. Volkov, Phys. Rep. **44**, 93 (1978).
- <sup>10</sup>J. Barrette, P. Braun-Münzinger, C. K. Gelbke, H. E. Wegner, B. Zeidman, A. Gamp, H. C. Harney, and Th. Walcher, Nucl. Phys. **A279**, 125 (1977).
- <sup>11</sup>J. Wilczyński, Phys. Lett. **47B**, 484 (1973).